Acta Crystallographica Section D
Biological Crystallography
ISSN 0907-4449

Three-dimensional structural characterization of a novel *Drosophila melanogaster* acylphosphatase

Simone Zuccotti,[a] Camillo Rosano,[b] Matteo Ramazzotti,[c] Donatella Degl'Innocenti,[c] Massimo Stefani,[c] Giampaolo Manao[c] and Martino Bolognesi[a,b]*

[a]Department of Physics–INFM and Center of Excellence for Biomedical Research, University of Genova, Via Dodecaneso 33, 16132 Genova, Italy, [b]National Institute for Cancer Research (IST), X-ray Structural Biology Unit, Largo R. Benzi 10, 16132 Genova, Italy, and [c]Department of Biochemical Sciences, University of Firenze, Viale Morgagni 50, 50134 Florence, Italy

Correspondence e-mail: bolognes@fisica.unige.it

© 2004 International Union of Crystallography
Printed in Denmark – all rights reserved

Analysis of the *Drosophila melanogaster* EST database led to the discovery and cloning of a novel acylphosphatase. The *CG18505* gene coding for a new enzyme (AcPDro2) is clearly distinct from the previously described *CG16870Acyp* gene, which also codes for a *D. melanogaster* acylphosphatase (AcPDro). The putative catalytic residues, together with residues held to stabilize the acylphosphatase fold, are conserved in the two encoded proteins. Crystals of AcPDro2, which belong to the trigonal space group $P3_121$, with unit-cell parameters $a = b = 45.8$, $c = 98.6$ Å, $\gamma = 120^\circ$, allowed the solution of the protein structure by molecular replacement and its refinement to 1.5 Å resolution. The AcPDro2 active-site structure is discussed.

Received 11 February 2004
Accepted 23 March 2004

PDB Reference: AcpDro2, 1urr, r1urrsf.

1. Introduction

Acylphosphatase (AcP; EC 3.6.1.7) is a cytosolic enzyme (about 10 kDa) that is widespread in the eukaryotic and prokaryotic phyla (both mesophilic and extremophilic). AcP catalyses the hydrolysis of carboxyl–phosphate bonds in acylphosphates, such as carbamoylphosphate, 1,3-biphosphoglycerate and the β-aspartylphosphate intermediate formed by the action of membrane pumps (Nassi *et al.*, 1993; Stefani & Ramponi, 1995). AcP is widely distributed in many tissues of vertebrate species, in which it can be found mainly in the skeletal muscle and in the heart as muscle-type AcP (MT-AcP). It is also found in erythrocytes, brain and testis as (organ) common-type AcP (CT-AcP). The two isoforms share more than 50% amino-acid sequence identity, their sequences being essentially conserved among vertebrates. The biological role of AcPs is still a matter of debate, but studies on the hydrolysis of the phosphorylated intermediates of membrane Na^+/K^+ and Ca^{2+} ATPases suggest a possible role in controlling the flux of these ions through cell membranes (Stefani & Ramponi, 1995).

Site-directed mutagenesis and crystallographic analyses have suggested that the family-conserved residues Arg23 and Asn41 are responsible for the phosphate-binding and catalytic activity of AcPs (Degl'Innocenti *et al.*, 2003). The proposed mechanism suggests that Asn41 positions and activates a nucleophilic water molecule next to the substrate, followed by a substrate-assisted cleavage of the target carboxyl–phosphate bond (Stefani *et al.*, 1997; Pastore *et al.*, 1992; Thunnissen *et al.*, 1996; Rosano *et al.*, 2002).

The three-dimensional structures of horse MT-AcP and bovine CT-AcP have been determined by NMR and X-ray crystallography (PDB codes 1aps and 2acy, respectively); both isoenzymes display the typical α/β globular fold found in other phosphate-binding proteins (Pastore *et al.*, 1992; Thunnissen *et al.*, 1996). The same fold and catalytic residues are conserved in the AcP domain of the prokaryotic hydrogenase maturation factor HypF (Paschos *et al.*, 2001; Rosano *et al.*, 2002). It has recently been reported that under suitable destabilizing conditions horse muscle AcPs can aggregate *in vitro* into fibrillar assemblies typical of degenerative pathologies such as Alzheimer's and Parkinson's diseases (Chiti *et al.*, 1999, 2000, 2002).

A first *Drosophila melanogaster* AcP, named AcPDro1 (Celniker *et al.*, 2002), shows about 40% sequence identity to both human AcP isoenzymes (Pieri *et al.*, 1998). Analysis of the *D. melanogaster* expressed sequence tags (EST) database has subsequently allowed the discovery of additional putative AcP genes. The *CG18505* gene product is a protein (AcPDro2) that displays about 44% amino-acid sequence identity to AcPDro1 and about 40% sequence identity to both human AcPs.

2. Materials and methods

2.1. AcPDro2 crystal growth

Cloning, expression and purification of AcPDro2 was achieved as reported previously (Degl'Innocenti *et al.*, 2003). Native AcPDro2 was crystallized using the vapour-diffusion method. Droplets containing 1.0 µl reservoir solution (2.35 *M* ammonium sulfate, 0.1 *M* CHES pH 9.5) and 1.0 µl 13 mg ml^{-1} AcPDro2 solution in 0.01 *M* sodium acetate pH 4.5 were equilibrated against crystallization wells containing 600 µl reservoir solution. Cryopro-

 DOI: 10.1107/S0907444904006808

tectant solutions containing 2.6 *M* ammonium sulfate, 0.1 *M* CHES pH 9.5 and 15% glycerol or 15% ethylene glycol were used for data collection. Tentative AcPDro2 complex crystals were prepared by co-crystallization with 0.005 *M* adenosine 5′-(β,γ-imido)triphosphate (AMP-PNP) or by soaking in 0.01 *M* *p*-nitrophenyl phosphate (pNPP) solutions under conditions closely matching those of the native protein crystallizations.

2.2. Data collection, structure solution and refinement

X-ray diffraction data were collected at ESRF (Grenoble, France) beamlines ID14-1 and ID29 at 100 K. Data were integrated using *MOSFLM* (Leslie, 1992) and scaled using *SCALA* and *TRUNCATE* from the *CCP*4 suite (Collaborative Computational Project, Number 4, 1994; Table 1). AcPDro2 crystals belong to the trigonal space group $P3_121$ (or enantiomorph), with unit-cell parameters $a = b = 45.8$, $c = 98.6$ Å, $\gamma = 120^\circ$ and one molecule per asymmetric unit (55.2% solvent content). The three-dimensional structure of native AcPDro2 was solved by molecular-replacement methods with the program *AMoRe* (Navaza, 1994) using as a starting model the X-ray structure of the CT-AcP from bovine testis (Thunnissen *et al.*, 1996; PDB code 2acy). A suitable solution (CC = 45.0, $R = 44.5\%$) was determined at 3.5 Å resolution. Rigid-body refinement was performed with the program *REFMAC*5 (Murshudov *et al.*, 1997), lowering the *R*-factor value to 0.361 ($R_{\rm free}$ = 0.393) at 3.0 Å resolution. Atomic refinement with isotropic *B*-factor cycles and model inspection/correction using the program *O* (Jones *et al.*, 1991) were carried out until convergence was reached. Similar procedures were applied for the crystals of the two putative complexes (diffraction data at 1.60 and 1.95 Å for the putative AcPDro2–AMP-PNP and AcPDro2–pNPP, respectively). Data-collection and refinement statistics for native AcPDro2 are reported in Table 1.

3. Results and discussion

3.1. Overall structure

The AcPDro2 model is well defined in the electron density from residue Val2 to residue His98 for the native protein and for two putative complexes with *p*-nitrophenyl phosphate (pNPP) and with adenosine 5′-(β,γ-imido)triphosphate (AMP-PNP); the amino-acid sequence numbering in AcPDro2 is defined according to the bovine CT-AcP crystal structure described by Thunnissen *et al.* (1996). Although AcPDro2 was expected to bind pNPP and AMP-PNP, we did not find any specific binding of such molecules to the enzyme incubated with either compound, nor could significant structural differences from the native protein structure be recognized in their refined electron densities.

The AcPDro2 α/β-sandwich fold, with $\beta\alpha\beta\beta\alpha\beta$ secondary-structure composition (4-1-3-2-5 β-strand topology; Fig. 1) displays a twisted five-stranded β-sheet protected on one side by two α-helices and fully solvent-exposed on the other side. The six loops connecting the secondary-structure elements have been labelled L1–L6 from the N-terminus to the C-terminus (Rosano *et al.*, 2002). The dimensions of the AcPDro2 molecule are about 35 × 25 × 20 Å; no core cavities in the protein structure are left after the close packing of the two antiparallel α-helices against the inner face of the β-sheet.

Table 1
Data-collection and refinement statistics.

Values in parentheses are for the last resolution shell.

Beamline	ESRF ID29
Wavelength (Å)	0.933
Resolution range (Å)	39.5–1.50 (1.54–1.5)
Total No. reflections collected	123126
No. unique reflections	19859
Redundancy	6.2
Completeness (%)	98.7 (97.8)
$R_{\rm merge}$ (%)	4.7 (36.0)
$I/\sigma(I)$	17.15 (2.9)
Wilson plot *B* factor (Å^2)	29.5
Resolution range used for refinement (Å)	10–1.5
No. reflections used in refinement	18931
No. reflections used in test set	999
R factor (working set + test set)	0.163
R factor (working set)	0.160 (0.185)
$R_{\rm free}$	0.230 (0.253)
Overall *B* factor (Å^2)	26.9
E.s.u. based on free *R* value (Å)	0.079
E.s.u. based on maximum likelihood (Å)	0.047
Correlation coefficient ($F_o - F_c$)	0.965
Correlation coefficient (based on free test set)	0.934
No. water molecules	111
No. glycerol molecules	1
R.m.s.d. from ideal values	
Bond lengths (Å)	0.016
Bond angles (°)	1.512
General planes (Å)	0.015
Average *B* values (Å^2)	
Main-chain atoms	27.1
Side-chain atoms	33.3
Water molecules	47.0
Ramachandran plot†: residues in	
Most favoured regions	77 (88.5%)
Allowed regions	9 (10.3%)
Generously allowed regions	1 (1.1%)
Disallowed regions	0 (0%)

† Laskowski *et al.* (1993).

The structural superposition of AcPDro2 with bovine CT-AcP yields an r.m.s.d. of 0.99 Å calculated over 86 C_α atoms. The two structures differ mainly in the six N-terminal residues, which in the bovine AcP structure are hydrogen bonded to the N-terminal cap of the α2 helix. Such a conformational deviation is likely to be related to crystal contacts affecting the AcPDro2 N-terminal segment. The maximum deviation between the AcpDro2 and bovine CT-AcP structures occurs at residue Arg69 (5.30 Å); this residue is located next to a hydrophobic cluster built up of residues Ile70, Phe22, Trp64 and Leu65, which has a role in defining the L5-loop conformation.

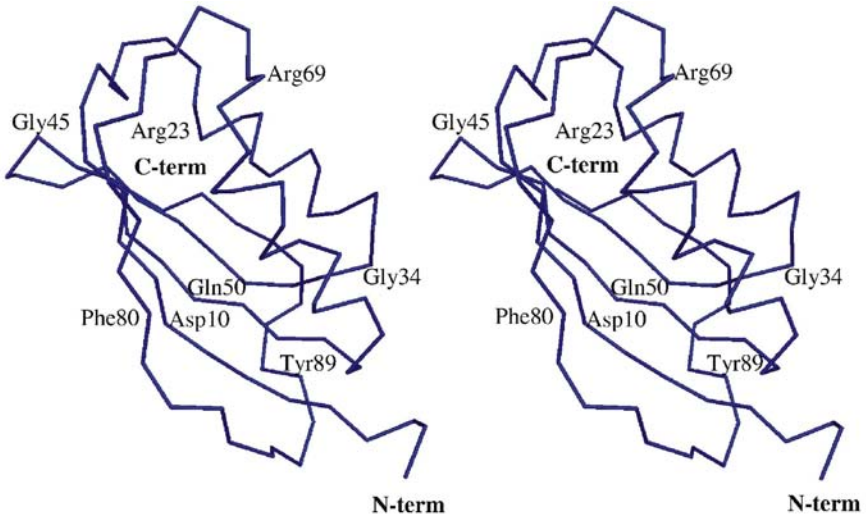

Figure 1
Stereoview of the AcPDro2 overall tertiary structure. N- and C-termini are labelled, together with selected residues.

3.2. Substrate-binding site

Comparison of the structure and sequence of AcPDro2 with those of the homologous mammalian AcPs allows the

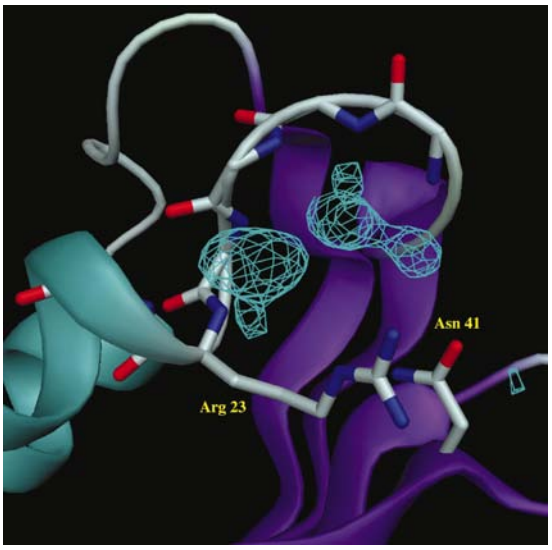

Figure 2
A view into the proposed AcPDro2 phosphate-binding site. The active-site residue and the main-chain atoms of the P-loop (residues 19–24) are reported together with a residual electron-density peak (see text for details).

identification of the phosphate-binding region of the protein as a cradle-like surface pocket built by the Gln18–Phe22 stretch close to the N-terminal region of the α1 helix (Fig. 2). The peptide N atoms of this stretch point towards the pocket centre where the phosphate moiety is expected to bind. Such a binding mode, previously observed for tetrahedral anions in CT-AcP (Thunnissen *et al.*, 1996), is reminiscent of that adopted by the low-molecular-weight phosphotyrosine protein phosphatases (LMW-PTPs; Su *et al.*, 1994; Ramponi & Stefani, 1997; Via et al., 2000).

The critical residues of the bovine CT-AcP active site (particularly Arg23 and Asn41) are conserved in AcPDro2, together with two active-site water molecules located in the region defined by the L1 and L3 loops and by the N-terminal region of the α1 helix. In MT-AcPs and CT-AcPs, the acylphosphatase activity has been proposed to rely on residue Arg23 (as the main substrate-binding site), as well as on residue Asn41 and on a hydrogen-bonded water molecule, which would act as a nucleophile when activated by the substrate, in a substrate-assisted catalytic mechanism (Thunnissen *et al.*, 1996). Remarkably, none of the AcpDro2 structures reported here displays a water molecule hydrogen bonded to Asn41, despite the ability of this enzyme to hydrolyse acylphosphates.

The AcPDro2 structure (as well as those of the two putative complexes) displays a broad active-site electron-density peak ($F_o - F_c$ map contoured at 3σ level) indicating orientational disorder of the bound species, which could be explained by a sulfate anion or glycerol molecule (in the purification buffer or in the cryoprotectant). It has been shown that human CT-AcP is able to catalyse the transfer of a phosphate group from pNPP to glycerol and that glycerol can enhance the acylphosphatase activity, as shown by the hyperbolic shape of the plot of k_{cat}/K_M against glycerol concentration (Paoli *et al.*, 2003). The same studies demonstrated that human CT-AcP may also hydrolyse arylphosphate monoesters *via* a mechanism that differs from that hypothesized for acylphosphates, in which a phosphate–enzyme intermediate would form at His25. It is worth noting that the residual electron density found in the AcPDro2 active site may fit a glycerol molecule in crystals treated with pNPP and AMP-PNP, as crystals of the native protein grown in the presence of glycerol or ethylene glycol display a more extended peak. Such observations would be in keeping with the idea that the enzyme can also hydrolyse both substrates in the crystalline state, while in the absence of the substrate a reaction intermediate, possibly formed by glycerol, phosphate or other reactants used in the purification stage, would be frozen in the active site. The presence of a bulky species in the active site could explain the observed lack of substrate binding by the AcPDro2 crystals and possibly the absence of the water molecule bound to Asn41.

This work has been supported by the FIRB grant RBAU015B47_002 (Protein Folding) to MB and FIRB grant RBNE01S29H_004 (Protein Misfolding and Human Pathologies) to MS. MB is grateful to Fondazione Compagnia di San Paolo (Torino) and to Istituto G. Gaslini (Genova) for continuous support.

References

Celniker, S. E. *et al.* (2002). *Genome Biol.* **3**, RESEARCH0079.
Chiti, F., Taddei, N., Baroni, F., Capanni, C., Stefani, M., Ramponi, G. & Dobson, C. M. (2002). *Nature Struct. Biol.* **9**, 137–143.
Chiti, F., Taddei, N., Bucciantini, M., White, P., Ramponi, G. & Dobson, C. M. (2000). *EMBO J.* **19**, 1441–1449.
Chiti, F., Webster, P., Taddei, N., Clark, A., Stefani, M., Ramponi, G. & Dobson, C. M. (1999). *Proc. Natl Acad. Sci. USA*, **96**, 3590–3594.
Collaborative Computational Project, Number 4 (1994). *Acta Cryst.* D**50**, 760–763.
Degl'Innocenti, D., Ramazzotti, M., Marzocchini, R., Chiti, F., Raugei, G. & Ramponi, G. (2003). *FEBS Lett.* **513**, 171–174.
Jones, T. A., Zou, J. Y., Cowan, S. & Kjeldgaard, M. (1991). *Acta Cryst.* A**47**, 110–119.
Leslie, A. G. W. (1992). *Jnt CCP4/ESF–EAMCB Newsl. Protein Crystallogr.* **26**, 27–33.
Laskowski, R. A., MacArthur, M. W., Moss, D. S. & Thornton, J. M. (1993). *J. Appl. Cryst.* **26**, 283–291.
Murshudov, G. N., Vagin, A. A. & Dodson, E. J. (1997). *Acta Cryst.* D**53**, 240–255.
Nassi, P., Nediani, C., Liguri, G., Taddei, N. & Ramponi, G. (1993). *Biochim. Biophys. Acta*, **1147**, 19–26.
Navaza, J. (1994). *Acta Cryst.* A**50**, 157–163.
Paoli, P., Pazzagli, L., Giannoni, E., Caselli, A., Manao, G., Camici, G. & Ramponi, G. (2003). *J. Biol. Chem.* **278**, 194–199.
Paschos, A., Glass, R. S. & Bock, A. (2001). *FEBS Lett.* **488**, 9–12.
Pastore, A., Saudek, B., Ramponi, G. & Williams, R. J. P. (1992). *J. Mol. Biol.* **224**, 427–440.
Pieri, A., Magherini, F., Liguri, G., Raugei, G., Taddei, N., Bozzetti, M. P., Cecchi, C. & Ramponi, G. (1998). *FEBS Lett.* **433**, 205–210.
Ramponi, G. & Stefani, M. (1997). *Biochem. Biophys. Acta*, **1341**, 137–156.
Rosano, C., Zuccotti, S., Bucciantini, M., Stefani, M., Ramponi, G. & Bolognesi, M. (2002). *J. Mol. Biol.* **321**, 785–796.
Stefani, M. & Ramponi, G. (1995). *Life Chem. Rep.* **12**, 271–301.
Stefani, M., Taddei, N. & Ramponi, G. (1997). *Cell Mol. Life Sci.* **53**, 141–151.
Su, X.-D., Taddeni, N., Stefani, M., Ramponi, G. & Nordlund, P. (1994). *Nature (London)*, **370**, 575–578.
Thunnissen, M. G. M., Taddei, N., Liguri, G., Ramponi, G. & Nordlund, P. (1996). *Structure*, **5**, 69–79.
Via, A., Ferre, F., Brannetti, B., Valencia, A. & Helmer-Citterich, M. (2000). *J. Mol. Biol.* **303**, 455–465.